

# An Acoustic Method for Flow Rate Estimation in Agricultural Sprayer Nozzles

Ruben Ruiz-Gonzalez <sup>a,\*</sup>, Timothy S. Stombaugh <sup>b</sup>, Víctor Martínez-Martínez <sup>a</sup>, and Jaime Gomez-Gil <sup>a</sup>

<sup>a</sup> Department of Signal and Communications Theory and Telematics Engineering, University of Valladolid, Valladolid 47011, Spain; E-Mail: jgomez@tel.uva.es (J.G.-G.), vmarmar@ribera.tel.uva.es (V.M.-M.);

<sup>b</sup> Biosystems and Agricultural Engineering Department, University of Kentucky, Lexington, KY 40546, USA; E-Mail: tim.stombaugh@uky.edu (T.S.);

\* Corresponding author; E-mail: rruigon@ribera.tel.uva.es; Tel.: +34-6366-81022; Fax: +34-9834-23667

---

**Abstract:** The cost of current flow rate measurement devices is quite high compared to the cost of low-end microphones. This circumstance, together with the fact that common agricultural sprayers have more than 50 nozzles, makes the use of current flow rate measurement devices cost-prohibitive. That considered, this article examines, by proposing one particular method, the feasibility of using microphones as flowmeters for nozzle tips in agricultural sprayers. The proposed method consists of the following stages: (i) acquisition of the digital acoustic data sequence, (ii) signal preprocessing, (iii) frequency domain transformation using FFT analysis, (iv) in-band power calculation, (v) power normalization, and (vi) regression or curve fitting. This method was assessed in an in-lab sprayer test bench employing 11 commercial nozzle tips at several operating flow rates. The experimental results yielded, for all the tested nozzle tips, average absolute and relative Root Mean Square Error (RMSE) values always below 0.08 liters per minute (lpm) and 5%, respectively, while the overall mean absolute and relative RMSE values were lower than 0.05 lpm and 2.5%. The accuracies when employing a high-end microphone instead of a low-end one were slightly worse, with a relative accuracy difference around 30%. These results provide strong evidence of the feasibility of accurately estimating the nozzle tip flow rate in real time based on acoustic signals. Moreover, no significant improvements are to be expected by using a high-end microphone instead of a low-end one. However, there are still some issues that should be tackled in order to enable the application of this method in real agricultural settings.

**Keywords:** agricultural sprayer nozzle; flowmeter; acoustic signal; microphone; frequency analysis; cost-effective solution.

---

## 1. Introduction

In the last few decades, agricultural sprayer technology has been continuously evolving toward the ability to accurately measure and control the flow rate of each individual nozzle on a spray boom [1, 2]. The recognition has been made that there can be significant variation between nozzles on a boom, and that the effects of vehicle turning maneuvers can be severely detrimental to achieve a uniform chemical application. By being able to control the flow rate of each individual nozzle, both a higher uniformity in turns and a more consistent application along straight paths can be achieved in the spread pattern of chemicals (pesticides, insecticides, fertilizers, and herbicides), which provides two distinct advantages. First, the reduction in the waste of chemicals would allow farmers to reduce the amount of chemicals used, thereby reducing production costs [3]. Second, in some applications the amount of chemicals to be dispatched is absolutely critical: when incorrect amounts are sprayed, either the chemicals will lack effectiveness because of under-application, or soil and crops will lose quality and yield, or they can be polluted and even irreversibly damaged, because of the over-application of chemicals [3-6].

48 To provide a finer resolution of control, solenoid-based electronic valves, controlled by  
49 *Pulse-Width Modulation (PWM)*, have been employed in agriculture at the nozzle level [7, 8]. The  
50 practical implementations of nozzle-level PWM control have been limited to open-loop control,  
51 which implicitly relies on uniformity and consistency of all the components across the boom for  
52 control accuracy. Feedback control would be much more accurate, but it would require reliable,  
53 real-time flow measurements from each nozzle. There is no currently available flow metering  
54 technology that could provide suitable accuracy at reasonable cost and size for implementation at  
55 each nozzle. The goal of this study is to develop an acoustic-based flow measuring technology that  
56 would be appropriate for implementation at the individual nozzle level to facilitate feedback  
57 control.

58 Many published articles have addressed the sound generation of nozzles and orifices [9-11].  
59 These studies have shown that the intensity and spectrum of the acoustic signal generated by  
60 nozzles and orifices change when the flow rate changes. Testud *et al.* [12, 13] investigated the sound  
61 generation by the presence of single-hole and multi-hole orifice plates along the pipe, showing that  
62 the characteristic whistling frequency of the emitted sound signal depends on the flow rate.  
63 Howe [14] showed that inner cavities in the pipe generate a sound signal whose acoustic intensity  
64 depends on the flow speed as a cubic function and whose cavity resonant tone frequency also  
65 depends on the speed of the stream flow. Druault *et al.* [15] also found a dependence of the acoustic  
66 signal spectrum on the flow rate due to the presence of a cavity along the pipe. Kobayashi *et al.* [16]  
67 studied, for an ocarina musical instrument, the dependence of the acoustic signal on the flow rate  
68 due to the presence of a cavity along the pipe.

69 Guided by the aforementioned research, the present study relies on the working hypothesis  
70 that flow rate changes through the sprayer nozzle tip will predictably change its generated acoustic  
71 signal both in intensity and frequency distribution. This hypothesis has already been proven valid in  
72 previous studies for taps or faucets [17, 18]. So far as the authors are aware, despite all the research  
73 advances, no prior progress has been made toward quantifying a relationship between the  
74 generated acoustic signal and the flow rate for sprayer nozzles. Thus, the proposal of this new  
75 acoustic flow rate estimation method is intended to become a point of inception for further research  
76 to gain more insight about flow rate estimation through acoustic signal processing.

77 The main goal of this article is to provide evidence supporting the feasibility of accurately  
78 estimating the flow rate of individual sprayer nozzles based on the acoustic signal measured close to  
79 the nozzle tip. To this end, four subobjectives can be highlighted: (i) the proposal of a new real-time  
80 flow rate estimation method based on the acoustic signal acquired by a nearby microphone, (ii) the  
81 assessment of this method's performance, (iii) the comparison of performance employing low-end  
82 versus high-end microphones, and (iv) the analysis of the influence of the nozzle-to-microphone  
83 distance on flow rate estimation.

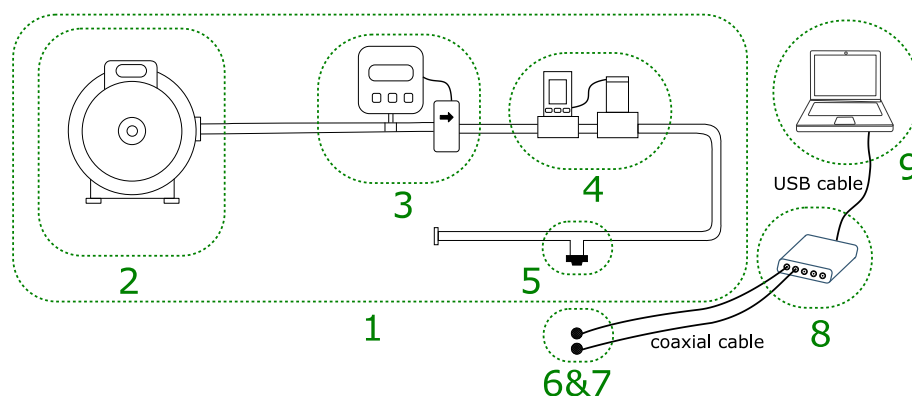
84 This article will describe the aforementioned proposed flow rate estimation method and  
85 highlight the Materials and Methods employed to undertake the research in this study (Section 2),  
86 present the main results obtained from the assessment of this method (Section 3), and present a  
87 discussion of this study's findings and conclusions (Sections 4 and 5).

## 88 2. Materials and Methods

89 All tests in this study were performed in a well-adapted laboratory belonging to the  
90 Department of Biosystems and Agricultural Engineering at the University of Kentucky in Lexington,  
91 KY, USA.

### 92 2.1. Materials

93

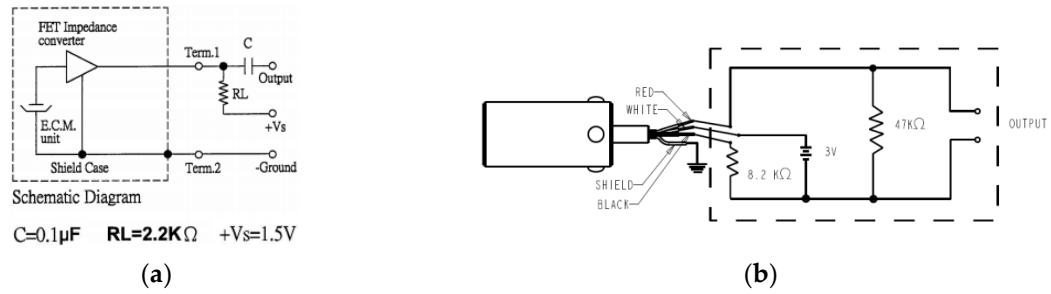


94 **Figure 1.** Schematic of the setup employed for conducting the experimental tests. The elements in the  
 95 schematic are: (1) sprayer test bench, (2) water tank and supply pump, (3) accurate reference  
 96 flowmeter, (4) flow controller, (5) nozzle mounting adapter and nozzle tips, (6&7) low-end and  
 97 high-end microphones, (8) data acquisition module, and (9) laptop computer.

98 The experimental setup used to conduct the experiments in this study consisted of the  
 99 following elements, where the item numbers in the list match the labels employed in Figure 1:

- 100 1. A laboratory sprayer test bench equipped with a water tank, a supply pump, hoses, pipes,  
 101 a flowmeter, a flow controller, and one nozzle mounting adapter.
- 102 2. A 200-liter water tank and a supply pump, which was composed of a *Dayton® 5K117BD*  
 103 industrial motor and an *Oberdorfer™ 101BM07MC* gear pump.
- 104 3. An *OMEGA Engineering Inc. FMG202-NPT* low-flow magnetic flowmeter, which was  
 105 employed to measure flow rates during the recording experiments to provide ground truth  
 106 reference for the evaluation of the proposed flow rate estimation method.
- 107 4. A *LCR-5LPM-D-100PSIG5V* liquid flow controller from *Alicat Scientific, Inc.*, which was  
 108 employed to control the flow rate at which water flowed through the nozzle tip.
- 109 5. A *Wilger Combo-Rate Modular Nozzle Body* that was used to mount the nozzle tips.–
- 110 6. A low-cost *CUI CMC-5044PF-A* electret microphone, plus preprocessing electronics. A  
 111 very simple electronic circuit (Figure 2a), which was specified by the manufacturer, was  
 112 used for impedance adaptation and high-pass filtering of the signal provided by the  
 113 microphone.
- 114 7. A high-end *Knowles BL-21994-000* microphone, plus preprocessing electronics, which was  
 115 used to check the results provided by the aforementioned low-end microphone. A very  
 116 simple electronic circuit (Figure 2b) was used for powering this microphone and setting its  
 117 proper operating point.
- 118 8. A *NI USB-4431* National Instruments (NI) data acquisition (DAQ) module, which was used  
 119 to digitize the signals provided by both analog microphone sensors.
- 120 9. A *Dell Latitude E6400* laptop computer, which was employed to acquire and save the  
 121 logged data coming from the data acquisition module. The connection between the laptop  
 122 and the data acquisition system was made through a USB cable. The laptop was also  
 123 employed to conduct the processing steps for the proposed flow rate estimation method,  
 124 as explained in Section 2.2.

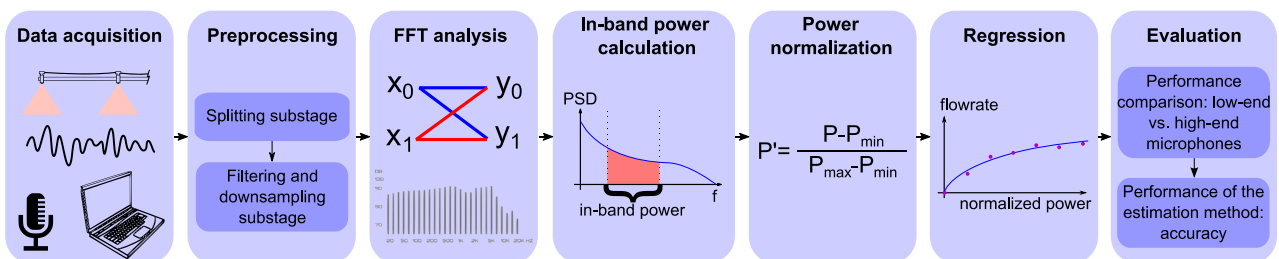
125 Eleven different agricultural nozzle tips were used in the experiments. These tips were chosen  
 126 among the most commonly used tips from two mainstream manufacturers: *TeeJet®* [19] and *Wilger*  
 127 *Industries Ltd* [20]. Specifically, from *TeeJet®*, the following set of nozzle tips was used: *AITT110-03*,  
 128 *AIX110-03*, *TG-03*, *Turbo TTVP110-03*, *TwinJet 80-03*, *XRC80-04*, and *XRC80-06*. From *Wilger*  
 129 *Industries Ltd*, the following *COMBO-JET®* nozzle tips were used: *ER80-03*, *MR80-04*, *MR80-06*, and  
 130 *MR80-08*. The chosen set of nozzle tips is considered representative enough, covering most of the  
 131 mainstream agricultural spraying applications, since they all present features differing in spray  
 132 pattern (flat fan, twin flat, and cone spray), droplet size (fine, medium, and coarse), spray fan angle  
 133 (80° and 110°), and flow rate operating range.



134 **Figure 2.** Schematic of the preprocessing electronic circuits for the: (a) *CUI CMC-5044PF-A*  
 135 microphone, and (b) *Knowles BL-21994-000* microphone.

## 136 2.2. Methods

137 The main processing stages performed in this study can be conceptualized as follows (Figure 3):  
 138 (i) data acquisition (Section 2.2.1); (ii) preprocessing (Section 2.2.2); (iii) FFT analysis (Section 2.2.3);  
 139 (iv) in-band power calculation (Section 2.2.4); (v) power normalization (Section 2.2.5); (vi) regression  
 140 or curve fitting (Section 2.2.6); and (vii) evaluation (Section 2.2.7). The first six stages correspond to  
 141 actual stages of the proposed flow rate estimation method, while the last one was aimed at assessing  
 142 the accuracy of this method. Figure 3 summarizes the main processing stages and contains an  
 143 overview of the methods, which are explained in greater detail in the remainder of this subsection.



144 **Figure 3.** Overall block diagram summarizing the main processing stages performed in this study.

### 145 2.2.1. Data acquisition

146 Acoustic data were experimentally obtained from around the nozzle by using the  
 147 aforementioned sprayer test bench. Both the low-end (*CUI CMC-5044PF-A*) and high-end (*Knowles*  
 148 *BL-21994-000*) microphones were used to measure the acoustic signal simultaneously. The location  
 149 of the microphones used for these recordings was as depicted in Figure 4. After several trial and  
 150 error tests, this location was considered the best for optimizing the overall method performance.  
 151 Two analog input channels of the National Instruments DAQ system, one for each microphone, were  
 152 employed using the *NI LabView* software running on the aforementioned laptop.

153 The acquisition experiments involved setting up a constant flow rate through the nozzle. Once  
 154 the flow rate had been stabilized, 61-second-long recordings were simultaneously taken with both  
 155 microphones using a sampling frequency of 100 kHz. Eleven different nozzle tips, previously  
 156 mentioned in Section 2.1, were tested. For each nozzle tip, several flow rates were used, all within or  
 157 close to the operating range recommended by the manufacturer in the respective product datasheet.  
 158 For each nozzle tip at each tested flow rate, two recordings were taken: one for training purposes  
 159 and the other for testing purposes. The training data were used to determine the parameters of the  
 160 subsequent processing stages of the estimation method. The testing data were used to assess the  
 161 performance of the method using these parameters.

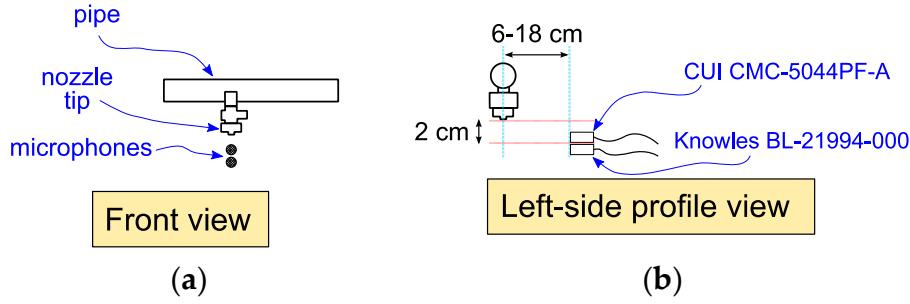


**Figure 4.** Location of the microphones with respect to the nozzle tip: (a) front view, and (b) left-side profile view.

162  
163

### 164 2.2.2. Preprocessing

165 The preprocessing stage consisted of two substages: (i) the splitting substage, and (ii) the  
166 filtering and downsampling substage. This stage was applied to each of the aforementioned  
167 61-second-long acquired signals, i.e., for all the recordings.

168 In the splitting substage, the complete 61-second-long sequence was divided into 122 epochs of  
169 0.5 seconds each. In order to achieve a real-time flow rate estimation, this time was empirically  
170 considered as the minimum epoch size able to prevent the loss of meaningful information from the  
171 acoustic signal. Thus, the subsequent stages are still able to accurately compute flow rates from this  
172 split signal.

173 In the filtering and downsampling substage, a digital IIR elliptic low-pass filter with a cutoff  
174 frequency of 4 kHz was applied to the split signal to avoid spectral aliasing in the subsequent  
175 downsampling stage. This cutoff frequency was chosen since all frequencies of interest for this  
176 method lie in a band below 2 kHz, as will be further detailed in Section 2.2.4. After the filtering, the  
177 signal was also downsampled by a factor of  $M = 10$ , to reduce its original length, thus avoiding  
178 unnecessary processing overload in terms of computational complexity. In this way, every 0.5  
179 seconds the subsequent FFT analysis stage receives as input the preprocessed data from one of these  
180 0.5-second-long epochs, consisting of  $N = 5,000$  samples. By doing so, the whole flow rate  
181 estimation method is able to update the provided measurement twice every second.

### 182 2.2.3. FFT analysis

183 In this stage the *Discrete Fourier Transform* (DFT) of each of the epochs was calculated using the  
184 *Fast Fourier Transform* (FFT) algorithm. Assuming that  $x[n]$ , with  $n \in \mathbb{Z}$  and  $n \in [0, N - 1]$ , denotes  
185 the discrete-time signal associated with each epoch output from the previous stage, its DFT  
186 transform,  $X[k]$ , is computed using Equation (1):

$$X[k] = \sum_{n=0}^{N-1} x[n] \cdot e^{-i \cdot 2\pi \cdot k \cdot n / N}, \text{ for } k = 0, \dots, N - 1 \quad (1)$$

187 After this step, the *Power Spectral Density* (PSD) was calculated using Equation (2):

$$PSD[k] = 2 \cdot \frac{X[k] \cdot X^*[k]}{N \cdot f_s} \quad (2)$$

188 where  $f_s = 10,000$  Hz is the effective sampling frequency after the downsampling by a factor of ten,  
189  $N$  is the length of the discrete signal  $X[k]$ , and the asterisk symbol denotes the complex conjugate of  
190 a complex number.

### 191 2.2.4. In-band power calculation

192 After having computed the PSD from the frequency spectrum via the FFT transform, the  
193 in-band power contained between 1,450 and 1,950 Hz was calculated by using the trapezoidal  
194 integration rule (Equation (3)). This frequency band was chosen after being considered the most  
195 suitable for the subsequent flow rate estimation. The process that led to this choice was a trial and

196 error approach constrained by the early observation of the frequency spectrum of the acoustic signal  
197 coming from the nozzle tip.

$$P = \sum_{k=725}^{974} \frac{PSD[k] + PSD[k + 1]}{2} \cdot 2 \text{ Hz} \quad (3)$$

198 In Equation (3),  $k = 725$  and  $k = 974$  are, respectively, the indexes corresponding to the 1,450  
199 and 1,948 Hz frequencies, since the employed frequential resolution was 2 Hz.

#### 200 2.2.5. Power normalization

201 The output from the previous stage, namely the unnormalized in-band power, became the  
202 input to this stage. The normalization process consisted of applying a linear mapping so that the  
203 output of this stage,  $P_{norm}$ , i.e. the normalized in-band power, was a value bounded between 0 and  
204 1. The zero and one values correspond, respectively, to the minimum and maximum tested flow  
205 rates of the particular nozzle tip assessed. Additionally, during the training phase in this stage, the  
206 values of  $P_{min}$  and  $P_{max}$  were obtained, once again individually for each assessed nozzle tip, as the  
207 mean in-band power of the 122 epochs for the minimum flow rate and for the maximum flow rate,  
208 respectively. The normalized power,  $P_{norm}$ , was calculated from the unnormalized power,  $P$ , using  
209 the following linear mapping (Equation (4)):  
210

$$P_{norm} = \frac{P - P_{min}}{P_{max} - P_{min}} \quad (4)$$

211

#### 212 2.2.6. Regression or curve fitting

213 After computing the normalized in-band power, for the training data for which the actual flow  
214 rate was known, the flow rate versus the normalized in-band power was plotted. Using a sixth root  
215 function, as shown in Equation (5), the parameters  $k_1$  and  $k_2$  were adjusted for each assessed  
216 nozzle tip to better fit the empirical training data points by means of a transformed linear regression  
217 using the least squares approach. The fitted data curve was later used for flow rate estimation with  
218 the new testing data so that the output of this stage was an estimate of the volumetric flow rate  
219 measured in liters per minute (lpm).

220 The aforementioned sixth root function employed in this stage was:

$$x = (k_1 + k_2 \cdot P_{norm})^{1/6} \quad (5)$$

221 where  $x$  denotes the flow rate output,  $P_{norm}$  is the normalized in-band power coming from the  
222 previous stage, and  $k_1$  and  $k_2$  are constants determined during the curve fitting stage with the  
223 training data set.

224 For calibration purposes, whenever the nozzle tip or nozzle-to-microphone distance changes,  
225 all the stages described between Section 2.2.1 and Section 2.2.6 should be conducted again while the  
226 actual flow rate is measured simultaneously with an accurate flowmeter. In this way, a new different  
227 curve is fitted in order to be used for later estimation.

#### 228 2.2.7. Evaluation

229 After having undertaken all the previous stages, the performance of the proposed method was  
230 assessed. For each nozzle tip, after performing the corresponding training phase, the method  
231 accuracy was evaluated for the testing data set. The evaluation stage consisted of using as input new  
232 acoustic signals and evaluating how accurate the method was in providing an estimate of the actual  
233 flow rate, which was measured concurrently with the accurate flowmeter. The absolute and relative  
234 *Root Mean Square Error* (RMSE), the maximum absolute error, and the 95% interpercentile range, as  
235 well as visual inspection, were used as performance metrics for evaluation.

236 The absolute and relative RMSE, the maximum absolute error, and the 95% interpercentile  
 237 range values were calculated for all the aforementioned testing data experiments, i.e. one for each  
 238 tested nozzle tip at several constant flow rates, as shown in Equations (6) to (9):

$$\text{Absolute RMSE} = \sqrt{\frac{1}{N} \sum_{i=1}^N (x_i - x_{GT})^2} \quad (6)$$

$$\text{Relative RMSE} = \frac{\sqrt{\frac{1}{N} \sum_{i=1}^N (x_i - x_{GT})^2}}{x_{GT}} = \frac{\text{Absolute RMSE}}{x_{GT}} \quad (7)$$

$$\text{maximum absolute error} = \max_{1 \leq i \leq N} \{|x_i - x_{GT}|\} \quad (8)$$

$$95\% \text{ interpercentile range} = 97.5\text{th percentile} - 2.5\text{th percentile} \quad (9)$$

239 where  $x_i$  is the estimated flow rate value obtained by the proposed method at the  $i$ -th epoch,  $x_{GT}$  is  
 240 the ground truth reference value provided by the accurate flowmeter, and  $N = 122$  denotes the  
 241 number of epochs for each experiment at a constant flow rate.

242 The assessment of the method, using the metrics previously introduced, consisted of three main  
 243 evaluation experiments: (i) one for the accuracies of all tested nozzle tips, (ii) another for the  
 244 influence of the quality of the measuring microphone, and (iii) a last one for the dependency on the  
 245 location of the microphone.

246 In the first evaluation experiment, just the low-end microphone (*CUI CMC-5044PF-A*) was  
 247 employed and it was located 6 cm from the nozzle tip (Figure 4). In this experiment, all 11 nozzle tips  
 248 were tested and compared for several flow rates lying within or close to their manufacturer  
 249 recommended operating ranges.

250 In the second evaluation experiment, both the high-end (*Knowles BL-21994-000*) and low-end  
 251 (*CUI CMC-5044PF-A*) microphones were used, once again placed 6 cm from the nozzle tip (Figure 4).  
 252 In order to report simpler results, three representative and commonly used nozzle tips were selected  
 253 for comparison: *TeeJet® XRC80-04*, *Wilger COMBO-JET® MR80-04*, and *TeeJet® AIX110-03*. In addition  
 254 to the aforementioned performance metrics, the correlation coefficients between the estimated flow  
 255 rate discrete-time sequences for both the high-end and low-end microphones were computed. This  
 256 value was used as a measurement of the coherence between the estimates provided by both  
 257 microphones.

258 In the third evaluation experiment, once again just the low-end microphone (*CUI*  
 259 *CMC-5044PF-A*) was employed, but several recordings were taken varying the  
 260 nozzle-to-microphone separation distances to 6, 12, and 18 cm. In order to report simpler results, just  
 261 one of the most commonly used nozzle tips was selected for comparison: *Wilger COMBO-JET®*  
 262 *MR80-04*. The aforementioned performance metrics were computed for the recordings at these three  
 263 separation distances in order to assess the influence of the distance on the method accuracy.

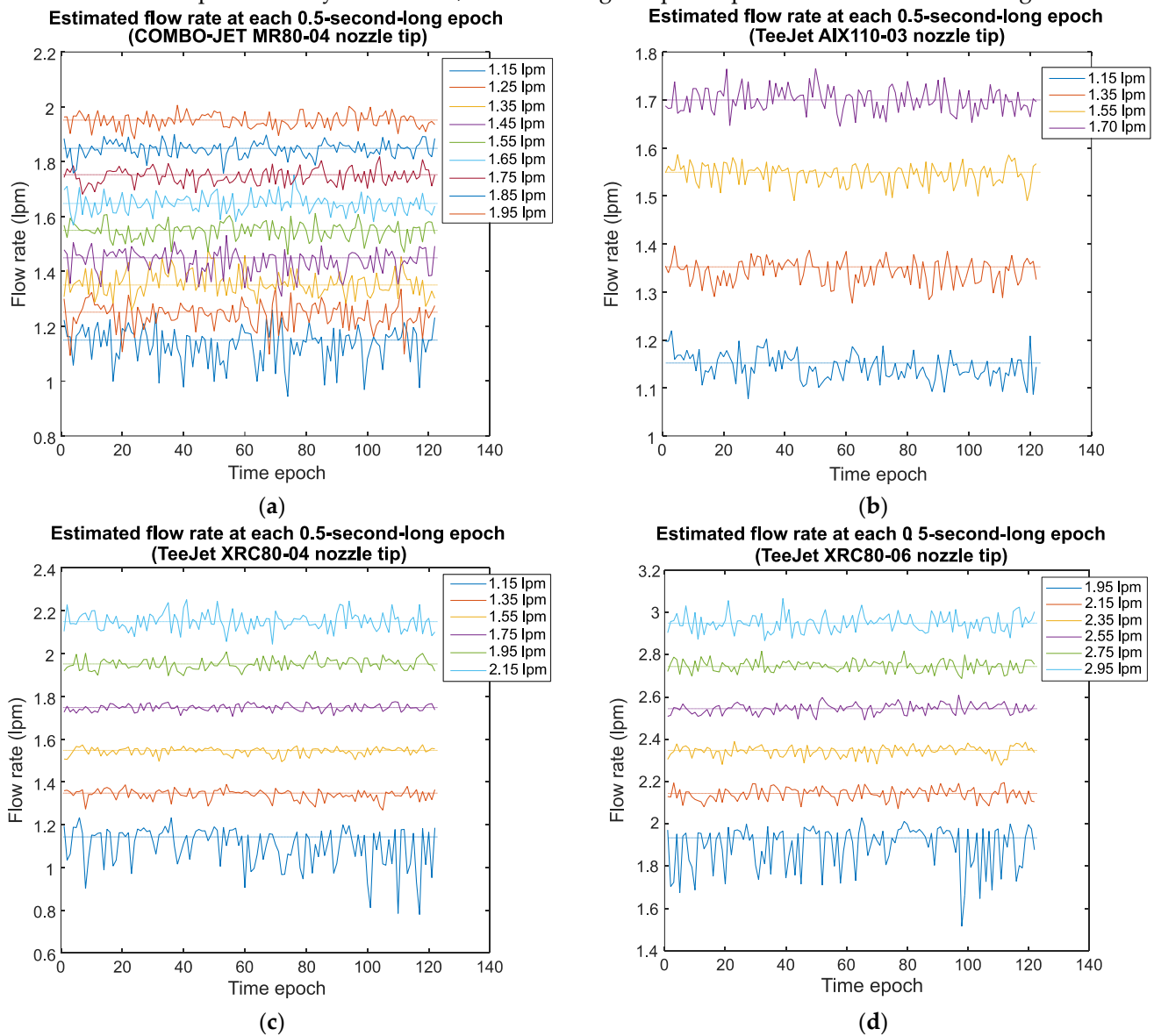
### 264 3. Results

265 For the sake of clarity, the main results of this study are presented in three separate subsections  
 266 corresponding to each of the aforementioned evaluation experiments (Section 2.2.7). First, the  
 267 estimation accuracy for all the tested nozzle tips was assessed. Second, the influence of the quality of  
 268 the measuring microphone was evaluated. Last, the dependency on the location of the microphone  
 269 was examined.

#### 270 3.1. Accuracy Results for Different Nozzle Tips

271 In this subsection, the accuracy results obtained with the 11 aforementioned nozzle tips (Section  
 272 2.1) are reported while using the low-end microphone (*CUI CMC-5044PF-A*).

273 Figure 5 depicts the flow rate discrete-time sequences estimated by the proposed method  
 274 applied to four acquired, representative acoustic signals for each of the 122 0.5-second-long epochs.  
 275 It can be seen that the proposed method makes real-time flow rate estimation possible, since the flow  
 276 rate can be updated every 0.5 seconds, thus allowing for quick updates as the flow rate changes.



277 **Figure 5.** Flow rate estimation results for each of the 122 0.5-second-long epochs while the flow rate  
 278 was kept constant and the low-end microphone (*CUI CMC-5044PF-A*) was 6 cm from the nozzle tip.  
 279 (a) *Wilger COMBO-JET® MR80-04* nozzle tip. (b) *TeeJet® AIX110-03* nozzle tip. (c) *TeeJet® XRC80-04*  
 280 nozzle tip. (d) *TeeJet® XRC80-06* nozzle tip.

281 Table 1 reports the accuracies for all 11 tested nozzle tips. It can be seen that the average values  
 282 for the absolute RMSE, the maximum absolute error, and the 95% interpercentile range of the error  
 283 are always below 0.08, 0.32 and 0.31 liters per minute (lpm), respectively. Computing the relative  
 284 RMSE, found by dividing the absolute RMSE by the actual flowrate, an average error always lower  
 285 than 5% was obtained for every single nozzle. These facts provide strong evidence of the usefulness  
 286 of the here-proposed flow rate estimation method, which led to high accuracies for all tested nozzle  
 287 tips.

288 **Table 1.** Accuracy results of the proposed flow rate estimation method for the tested nozzle tips and  
 289 flow rates using the low-end microphone (*CUI CMC-5044PF-A*).



Nozzle tip employed	Actual flow rate (lpm)	Absolute RMSE (lpm)	Relative RMSE (%)	Maximum absolute error (lpm)	95% interpercentile range (lpm)
Wilger COMBO-JET® MR80-04	1.15	0.0689	5.991	0.2065	0.2550
	1.25	0.0487	3.896	0.1570	0.2201
	1.35	0.0455	3.370	0.1291	0.1695
	1.45	0.0462	3.186	0.1407	0.1626
	1.55	0.0318	2.052	0.0887	0.1353
	1.65	0.0331	2.006	0.1028	0.1228
	1.75	0.0280	1.600	0.0688	0.1053
	1.85	0.0280	1.514	0.0925	0.1150
	1.95	0.0262	1.344	0.0667	0.1010
	<b>Average</b>	<b>0.0396</b>	<b>2.773</b>	<b>0.1170</b>	<b>0.1541</b>
Wilger COMBO-JET® MR80-06	1.92	0.0921	4.797	0.3008	0.2914
	2.12	0.0434	2.047	0.1267	0.1699
	2.31	0.0511	2.212	0.1188	0.1804
	2.49	0.0406	1.631	0.0935	0.1578
	2.68	0.0413	1.541	0.1128	0.1594
	2.87	0.0446	1.554	0.1043	0.1757
	<b>Average</b>	<b>0.0439</b>	<b>2.297</b>	<b>0.1205</b>	<b>0.1618</b>
Wilger COMBO-JET® MR80-08	2.57	0.1221	4.751	0.4658	0.4277
	2.77	0.0382	1.379	0.1207	0.1475
	2.96	0.0539	1.821	0.1493	0.2271
	3.16	0.0463	1.465	0.1297	0.1898
	3.34	0.0483	1.446	0.1095	0.1699
	3.53	0.0490	1.388	0.1474	0.2004
	3.72	0.0451	1.212	0.1111	0.1818
	3.92	0.0436	1.112	0.1233	0.1796
	4.12	0.0575	1.396	0.1704	0.2148
	<b>Average</b>	<b>0.0560</b>	<b>1.775</b>	<b>0.1697</b>	<b>0.2154</b>
TeeJet® AIX110-03	1.15	0.0289	2.513	0.0726	0.1094
	1.35	0.0263	1.948	0.0733	0.0956
	1.55	0.0220	1.419	0.0602	0.0815
	1.70	0.0255	1.500	0.0658	0.0931
		<b>Average</b>	<b>0.0257</b>	<b>1.845</b>	<b>0.0680</b>
TeeJet® Turbo TTVP110-03	1.15	0.0239	2.078	0.0634	0.0980
	1.35	0.0316	2.340	0.0695	0.1232
	1.55	0.0349	2.252	0.0937	0.1418
	1.73	0.0545	3.150	0.1409	0.2231
		<b>Average</b>	<b>0.0362</b>	<b>2.455</b>	<b>0.0919</b>

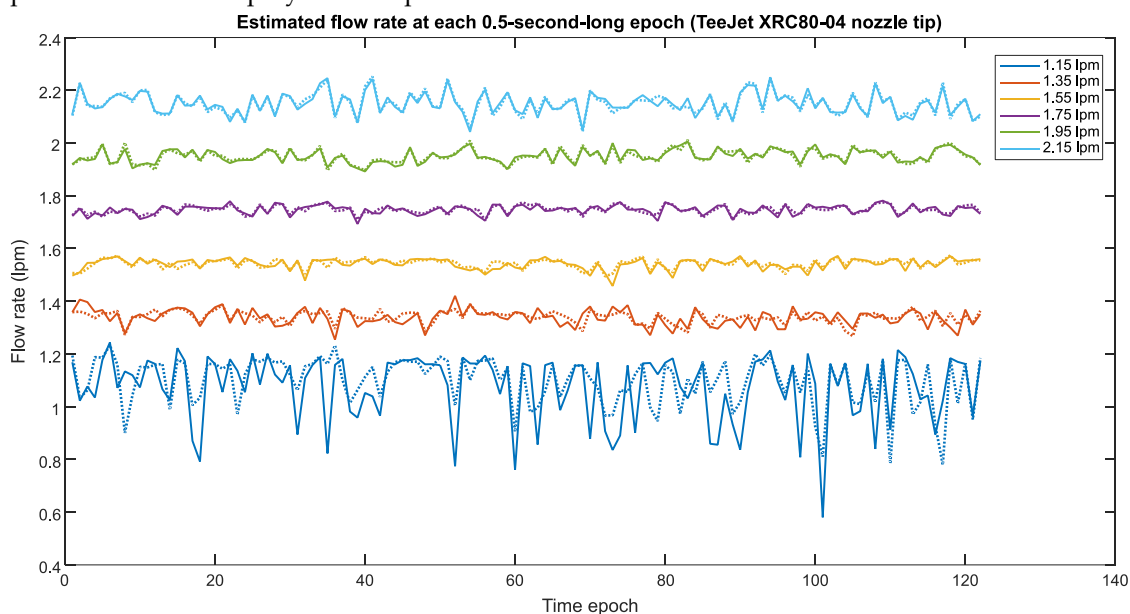
	1.55	0.1337	8.626	0.6491	0.5191
TeeJet®	1.75	0.0568	3.246	0.1639	0.2324
AITT110-03	1.95	0.0433	2.221	0.1195	0.1708
	<b>Average</b>	<b>0.0779</b>	<b>4.697</b>	<b>0.3108</b>	<b>0.3074</b>
	1.55	0.0750	4.839	0.1830	0.3041
	1.75	0.0668	3.817	0.1664	0.2697
TeeJet® TG-03	1.95	0.0598	3.067	0.1675	0.2411
	2.15	0.0435	2.023	0.1320	0.1603
	2.35	0.0451	1.919	0.1397	0.1862
	<b>Average</b>	<b>0.0580</b>	<b>3.133</b>	<b>0.1577</b>	<b>0.2323</b>
	1.15	0.0267	2.322	0.0806	0.1010
TeeJet®	1.35	0.0277	2.052	0.0664	0.1033
TwinJet 80-03	<b>Average</b>	<b>0.0272</b>	<b>2.187</b>	<b>0.0735</b>	<b>0.1022</b>
	0.95	0.0651	6.853	0.2139	0.1990
Wilger	1.15	0.0162	1.409	0.0611	0.0586
COMBO-JET®	1.35	0.0232	1.719	0.0623	0.0912
ER80-03	1.55	0.0621	4.006	0.2014	0.2357
	<b>Average</b>	<b>0.0416</b>	<b>3.497</b>	<b>0.1347</b>	<b>0.1461</b>
	1.95	0.1168	5.990	0.4338	0.3296
	2.15	0.0306	1.423	0.0789	0.1089
TeeJet®	2.35	0.0252	1.072	0.0729	0.0969
	2.55	0.0236	0.925	0.0595	0.0851
XRC80-06	2.75	0.0269	0.978	0.0682	0.0978
	2.95	0.0405	1.373	0.1158	0.1557
	<b>Average</b>	<b>0.0446</b>	<b>1.960</b>	<b>0.1427</b>	<b>0.1437</b>
	1.15	0.1065	9.261	0.3709	0.3372
	1.35	0.0254	1.881	0.0823	0.0924
TeeJet®	1.55	0.0189	1.219	0.0557	0.0638
	1.75	0.0163	0.931	0.0439	0.0595
XRC80-04	1.95	0.0257	1.318	0.0613	0.1019
	2.15	0.0423	1.967	0.1063	0.1644
	<b>Average</b>	<b>0.0386</b>	<b>2.763</b>	<b>0.1228</b>	<b>0.1310</b>

### 290 3.2. Accuracy Comparison of High-End versus Low-End Microphones

291 In this subsection, a performance comparison between low-end and high-end microphones is  
292 tackled for the proposed flow rate estimation method. In order to simplify the comparison of the  
293 results from the two different microphones, only three representative nozzle tips were selected:  
294 *TeeJet® XRC80-04*, *Wilger COMBO-JET® MR80-04*, and *TeeJet® AIX110-03*. As previously noted, the  
295 same experiments were simultaneously recorded with both microphones for a more unbiased  
296 accuracy comparison between them.

297 Figure 6 shows a comparison of the estimated flow rate discrete-time sequences for all 122  
298 0.5-second-long epochs with both microphones for the *TeeJet® XRC80-04* nozzle tip. A very high  
299 similarity is observed for the highest flow rates, while small discrepancies appear for the lowest flow  
300 rates. This plot is a proof of the high coherence between the measurements provided by both

301 microphones, which highlights the consistency of the here-proposed method with almost no  
 302 dependence on the employed microphone.



303 **Figure 6.** Comparison of the flow rate estimation results for each of the 122 0.5-second-long epochs  
 304 while the flow rate was kept constant and the microphones were 6 cm from the *TeeJet*<sup>®</sup> XRC80-04  
 305 nozzle tip. The solid and dotted lines represent the results for the high-end microphone (*Knowles*  
 306 *BL-21994-000*) and the low-end microphone (*CUI CMC-5044PF-A*), respectively.

307 Table 2, Table 3, and Table 4 show the results obtained while using the high-end microphone  
 308 (*Knowles BL-21994-000*) instead of the low-end one (*CUI CMC-5044PF-A*). A comparison between the  
 309 performance for the *TeeJet*<sup>®</sup> XRC80-04 nozzle tip in Table 1 and Table 2 reveals that the high-end  
 310 microphone does not outperform the low-end microphone. In fact, the accuracies were slightly  
 311 worse for the high-end microphone. The same conclusion can be reached by comparing the results  
 312 for the *Wilger COMBO-JET*<sup>®</sup> MR80-04 and *TeeJet*<sup>®</sup> AIX110-03 nozzle tips in Table 1 with the results in  
 313 Table 3 and Table 4, respectively. This fact proves that highly accurate results can be achieved with a  
 314 low-end microphone, with no significant improvements expected when using a high-end one.  
 315 Another remarkable result is that moderate (0.40-0.59) to very strong (0.80-1.00) correlations are  
 316 observed between the measurements provided by both microphones. This fact clearly highlights the  
 317 existence of a significant coherence between the measurements provided by both devices.

318 **Table 2.** Accuracy results of the proposed flow rate estimation method for the *TeeJet*<sup>®</sup> XRC80-04  
 319 nozzle tip employing the high-end microphone (*Knowles BL-21994-000*).

Actual flow rate (lpm)	Absolute RMSE (lpm)	Maximum absolute error (lpm)	95% interpercentile range (lpm)	Correlation coefficient
1.15	0.1467	0.5696	0.4300	0.6065
1.35	0.0334	0.0958	0.1214	0.6574
1.55	0.0223	0.0920	0.0779	0.8284
1.75	0.0182	0.0568	0.0698	0.8880
1.95	0.0254	0.0579	0.0926	0.9531
2.15	0.0415	0.1077	0.1633	0.9700
<b>Average</b>	<b>0.0479</b>	<b>0.1633</b>	<b>0.1592</b>	<b>0.8172</b>

320  
321**Table 3.** Accuracy results of the proposed flow rate estimation method for the *Wilger COMBO-JET*<sup>®</sup> *MR80-04* nozzle tip employing the high-end microphone (*Knowles BL-21994-000*).

Actual flow rate (lpm)	Absolute RMSE (lpm)	Maximum absolute error (lpm)	95% interpercentile range (lpm)	Correlation coefficient
1.15	0.1274	0.2119	0.3314	0.4103
1.25	0.0786	0.1821	0.2429	0.5084
1.35	0.0746	0.1878	0.2574	0.4996
1.45	0.0842	0.1941	0.2522	0.5489
1.55	0.0723	0.1787	0.2881	0.6093
1.65	0.0645	0.1799	0.2373	0.6910
1.75	0.0512	0.1796	0.2014	0.6188
1.85	0.0442	0.1308	0.1796	0.6114
1.95	0.0516	0.1346	0.2071	0.6583
<b>Average</b>	<b>0.0721</b>	<b>0.1755</b>	<b>0.2442</b>	<b>0.5729</b>

322  
323**Table 4.** Accuracy results of the proposed flow rate estimation method for the *TeeJet*<sup>®</sup> *AIX110-03* nozzle tip employing the high-end microphone (*Knowles BL-21994-000*).

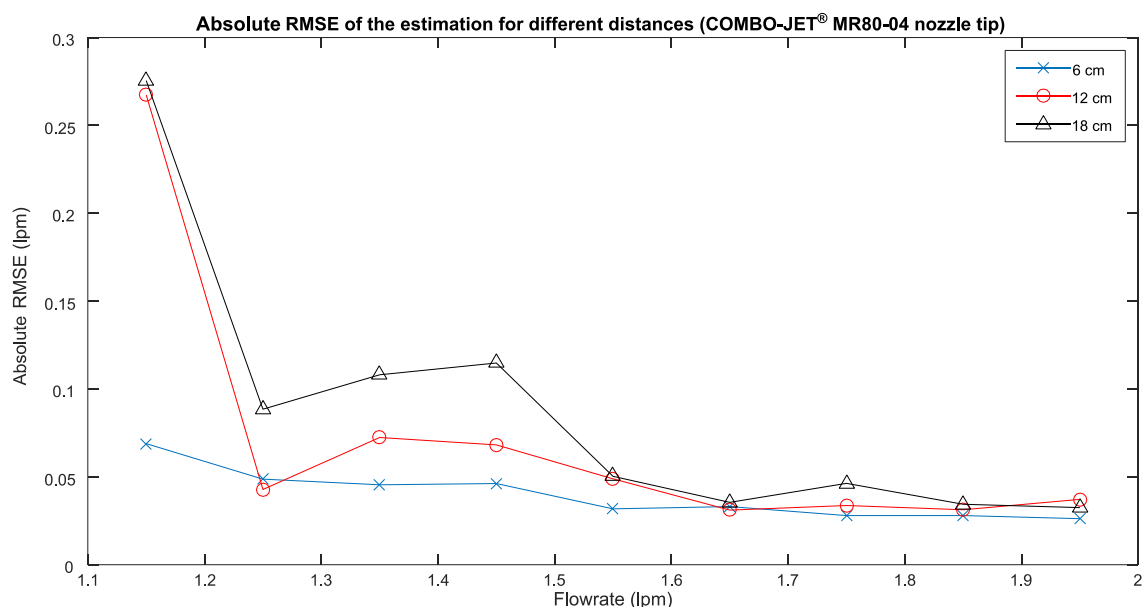
Actual flow rate (lpm)	Absolute RMSE (lpm)	Maximum absolute error (lpm)	95% interpercentile range (lpm)	Correlation coefficient
1.15	0.0439	0.1179	0.1887	0.4996
1.35	0.0311	0.1038	0.1178	0.5084
1.55	0.0290	0.0785	0.1030	0.7467
1.70	0.0282	0.0687	0.1154	0.8020
<b>Average</b>	<b>0.0331</b>	<b>0.0922</b>	<b>0.1312</b>	<b>0.6392</b>

324 **3.3. Accuracy Comparison for Different Nozzle-to-Microphone Distances**

325 In this subsection, an accuracy comparison of the proposed method for different  
326 nozzle-to-microphone separation distances is provided while using the low-end microphone (*CUI*  
327 *CMC-5044PF-A*).

328 Table 5 shows the accuracies for the *Wilger COMBO-JET*<sup>®</sup> *MR80-04* nozzle tip at different  
329 distances: 6, 12, and 18 cm. Figure 7 shows the absolute RMSE of the estimation for different flow  
330 rates at the three tested distances. In general, a gradual degradation of the accuracy can be observed  
331 as distance is increased. This degradation is higher for the lowest flow rates, probably due to the fact  
332 that the generated signal has less intensity and the acoustic noise floor masks the signal of interest.  
333 Nevertheless, this degradation is almost negligible for the rest of the higher flow rates, as long as the  
334 distances are kept close enough.

335



336  
337  
338

**Figure 7.** Comparison of the absolute RMSE estimation accuracy at several flow rates for different nozzle-to-microphone distances using the *Wilger COMBO-JET® MR80-04* nozzle tip and the low-end microphone (*CUI CMC-5044PF-A*).

339  
340

**Table 5.** Accuracy results for the *Wilger COMBO-JET® MR80-04* nozzle tip using the low-end microphone (*CUI CMC-5044PF-A*) at different distances.

Distance from nozzle tip to microphone	Actual flow rate (lpm)	Absolute RMSE (lpm)	Maximum absolute error (lpm)	95% interpercentile range (lpm)
6 cm	1.15	0.0689	0.2065	0.2550
	1.25	0.0487	0.1570	0.2201
	1.35	0.0455	0.1291	0.1695
	1.45	0.0462	0.1407	0.1626
	1.55	0.0318	0.0887	0.1353
	1.65	0.0331	0.1028	0.1228
	1.75	0.0280	0.0688	0.1053
	1.85	0.0280	0.0925	0.1150
	1.95	0.0262	0.0667	0.1010
	<b>Average</b>		<b>0.0396</b>	<b>0.1170</b>
12 cm	1.15	0.2674	0.6120	0.6815
	1.25	0.0428	0.1699	0.1382
	1.35	0.0724	0.1761	0.2682
	1.45	0.0682	0.1704	0.2696
	1.55	0.0489	0.1682	0.1617
	1.65	0.0311	0.1042	0.1278
	1.75	0.0337	0.1185	0.1302
	1.85	0.0313	0.0860	0.1127
	1.95	0.0372	0.1140	0.1543
	<b>Average</b>		<b>0.0703</b>	<b>0.1910</b>
18 cm	1.15	0.2755	0.5863	0.7789
	1.25	0.0885	0.3251	0.2738

1.35	0.1081	0.2134	0.2964
1.45	0.1148	0.2178	0.3070
1.55	0.0503	0.2163	0.2206
1.65	0.0355	0.1008	0.1369
1.75	0.0463	0.1435	0.1704
1.85	0.0344	0.0896	0.1359
1.95	0.0325	0.1034	0.1435
<b>Average</b>	<b>0.0873</b>	<b>0.2218</b>	<b>0.2737</b>

#### 341 4. Discussion

342 This article investigates the feasibility of using microphones as flowmeters for nozzle tips in  
 343 agricultural sprayers. For this end, a flow rate estimation method is proposed for each individual  
 344 nozzle tip by processing the generated acoustic signal acquired by a microphone located near the  
 345 nozzle. The main finding that can be drawn from this article is that accurate real-time flow rate  
 346 estimation for individual nozzle tips can be achieved by employing acoustic signal processing.

347 Seven major findings can be highlighted from this study: (i) the nozzle-generated acoustic  
 348 signal contains enough information to enable accurate flow rate estimation by applying signal  
 349 processing techniques; (ii) the proposed method can be used to estimate the flow rate of individual  
 350 nozzles in a low-cost way with a high accuracy in a laboratory environment; (iii) the flow rate  
 351 estimation becomes less accurate when operating outside the flow range recommended by the  
 352 nozzle manufacturer; (iv) the proposed method can be used to estimate the flow rate in real time  
 353 with a demonstrated update frequency of 2 Hz; (v) consistent results can be obtained when using a  
 354 low-end microphone instead of a more expensive high-end microphone; (vi) the frequency band  
 355 between 1,450 Hz and 1,950 Hz provided the best results; and (vii) the nozzle-to-microphone  
 356 distance is not critical for the method to work accurately, but specific calibrations are required for  
 357 each distance.

358 The first finding is that the nozzle-generated acoustic signal contains enough information to  
 359 enable accurate flow rate estimation. This general conclusion can be derived from the particular  
 360 results achieved with the proposed method. It is evident that the generated acoustic signal contains  
 361 information related to the flow rate through the nozzle tip, and many processing techniques can be  
 362 proposed for this end. Similar conclusions regarding this relationship have been found in previous  
 363 studies. Jacobs *et al.* [17] already proved that the sound of water flowing through a tap can be used to  
 364 estimate the actual flow rate. Kakuta *et al.* [18] demonstrated that a condenser microphone can be  
 365 used as a vibration sensor in pipelines in order to measure flow rates. Evans *et al.* [21] also employed  
 366 flow-induced mechanical vibrations in the pipe, acquired with an accelerometer, to estimate flow  
 367 rates. Nevertheless, the present article complements the aforementioned studies by addressing  
 368 sprayer nozzles where the flow is actually exiting a closed system in a controlled manner.

369 The second finding is that the proposed method can be used to estimate the flow rate of  
 370 individual nozzles in a low-cost way with a high accuracy in a laboratory environment. The results  
 371 presented in Section 3, mainly Table 1, support this finding, since for all the tested nozzles the  
 372 average absolute and relative RMSE values are always below 0.08 lpm and 5%, respectively.  
 373 Moreover, for flow rates lying within the manufacturer recommended operating ranges, the  
 374 absolute and relative RMSE values are even lower, bounded below 0.05 lpm and 2.5%, respectively.  
 375 Comparing these results with the ones obtained by Jacobs *et al.* [17], significantly better absolute  
 376 accuracies and slightly better relative accuracies are achieved with the here-proposed method.  
 377 However, it is worth noting that both studies are not quite comparable due to the nozzle tips versus  
 378 faucets or taps are and also flow rate ranges are very different in both articles. The flow rate  
 379 estimation accuracies obtained with the proposed acoustic method are close enough to some of the  
 380 traditionally used flowmeters, whose relative RMSE errors can reach 4% [22, 23]. Moreover, it is  
 381 commonly agreed, in mainstream agricultural spraying applications, that any flow rate variability  
 382 among nozzles below XXX% is acceptable for enabling precision agriculture spraying of chemicals.

383 Thus, the values obtained for relative RMSE error, all bounded below 5%, pose evidences of the  
384 validity of this measurement method to meet this requirement when used for flow rate control. It  
385 should be noted that these studies were conducted in a relatively controlled laboratory environment;  
386 thus, the reproducibility of these accuracies in real agricultural settings has yet to be verified.

387 The third finding is that the flow rate estimation becomes more difficult, i.e. the errors increase,  
388 for either very low or very high flow rates, when operating outside the flow range recommended by  
389 the nozzle manufacturer. This behavior can be noticed in Table 1 for almost every single nozzle. One  
390 possible explanation for this behavior is the fact that the spray deposition pattern and output droplet  
391 size distribution of the nozzles changes appreciably outside of the manufacturer recommended  
392 range, which will consequently change the acoustic signature. The higher difficulty in estimation  
393 could also be due to the acoustic signals being more similar in these extreme cases. This effect is even  
394 more noticeable for low flow rates due to the inherently lower intensity of the nozzle-generated  
395 signal. This lower intensity leads to the acoustic noise floor being relatively stronger with respect to  
396 the signal of interest, thus making the estimation more difficult. Nevertheless, it has been checked  
397 that, in the recommended operating flow rate ranges given by the nozzle manufacturers, the  
398 proposed method presents satisfactory accuracies. No similar findings about lower estimation  
399 capabilities for extreme flow rates have been detected in previous studies, to the best of the authors'  
400 knowledge. Further studies should be conducted to provide more insight regarding the reasons  
401 behind this behavior.

402 The fourth finding is that the proposed method can work in real time. This method, when  
403 executed in post-processing in MATLAB®, requires less than five seconds to process the  
404 61-second-long recordings for 10 flow rates, where the reported times were obtained in the  
405 aforementioned laptop (*Dell Latitude E6400*). This execution time, less than 0.01 seconds for each  
406 single epoch, shows the feasibility of performing all the necessary tasks between the acquisitions of  
407 two consecutive epochs, which is 0.5 seconds. It is worth remarking that no explicit code  
408 optimization was done and the computational efficiency of the method could be further improved  
409 for real-time operation.

410 The fifth finding is that consistent results, with neither significant improvements nor  
411 detriments, can be obtained when using a high-end or a low-end microphone. The results presented  
412 in Section 3.2 prove that the high-end microphone does not outperform the low-end microphone.  
413 Furthermore, the measurements provided by both are coherent (Figure 6), since moderate  
414 (0.40-0.59), strong (0.60-0.79) or very strong (0.80-1.0) positive correlations were found (Table 2,  
415 Table 3, and Table 4). The fact that the proposed method is highly independent of microphone  
416 quality makes it fiscally feasible to replicate flow sensors across a large boom with many nozzles.

417 The sixth finding is that the frequency band between 1,450 Hz and 1,950 Hz provided the best  
418 accuracies. Several bandwidths were tested, and a bandwidth of 500 Hz was found to be the best  
419 because it gave acceptable accuracies and was narrow enough to avoid excessive wideband  
420 interferences. Looking over the frequencies from 0 Hz to 50 kHz, the band from 1,450 Hz to 1,950 Hz  
421 contained more information than any other related to the flow rate.

422 The seventh finding is that the method accuracy does not depend too much on the  
423 nozzle-to-microphone distance. The results in Figure 7 and Table 5 show a tendency of a slow but  
424 progressive accuracy degradation as distance is increased. Only distances over 6 cm were tested in  
425 order to prevent the microphones from getting wet and thus being damaged. Moreover, since  
426 specific calibrations are required for each distance, it is worth noting that the proposed method will  
427 require strict control of microphone location while operating.

428 The major strength of the proposed method is the low-cost of its design, requiring for its  
429 deployment only a low-end microphone and a microcontroller-based computing platform. Another  
430 strength of the proposed estimation method is that it can work in real time.

431 Nevertheless, there are also some limitations to this work. Each nozzle tip requires its own  
432 calibration since no singular curve could be fitted accurately for all nozzle tips. Moreover, since the  
433 flow rate estimation method is dependent on the nozzle-to-microphone distance, as acoustic power  
434 decreases with distance, a new calibration process is mandatory when this distance is varied.

435 However, a simple straightforward calibration can be used in this case, requiring just the  
436 determination of the in-band power for highest and lowest flow rates for the normalization stage.

437 The low-cost sensing method evaluated in this study will bring tremendous benefits to the  
438 agricultural chemical application industry. It will be fiscally feasible to replicate this sensor at every  
439 nozzle along a large spray boom to facilitate monitoring and closed-loop control of flow rate from  
440 each individual nozzle tip. This will greatly increase the accuracy of placement of chemicals in the  
441 field and will prevent much of the errors and inconsistencies currently observed in field application  
442 equipment.

443 Future research related to this article could tackle the evaluation, and almost certainly  
444 improvement, of this method in real agricultural settings. More research on how to avoid acoustic  
445 interferences in real agricultural settings is needed as well. It is expected that interferences in real  
446 agricultural settings, e.g. acoustic noise generated by machinery and wind, can affect the  
447 performance of this method. The authors of this paper are currently undertaking new studies in this  
448 line of research.

449 Further studies are also required to gain more insight into where the sound enabling flow rate  
450 estimation comes from. Five possible sources for the generated acoustic signal have been identified  
451 while performing the experiments of this study: (i) turbulences generated by cavities inside the  
452 pipe-nozzle interface, (ii) droplet formation in the nozzle-air interface, (iii) acoustic radiation  
453 generated by mechanical vibrations of the nozzle or the pipe, (iv) residual elasticity of the nozzle tip  
454 outlet that makes its vibration dependent on the flow rate, which acts as an excitation force, (v) finite  
455 compressibility of the liquid, and (vi) cross section changes and presence of orifice plates along pipes  
456 or the nozzle. This article does not focus on identifying which of these sources have a predominant  
457 effect in the observed acoustic signature, but the authors of this paper are working on a follow-up  
458 study investigating the sound generation process for nozzle tips by using *Computational Fluids*  
459 *Dynamics (CFD)* simulations.

## 460 5. Conclusions

461 The results from this study support the feasibility of accurately estimating, in real time, the flow  
462 rate through agricultural sprayer nozzles based on the acoustic signal recorded in close proximity to  
463 them. While employing the proposed method, satisfactory accuracies with relative RMSE values  
464 below 5% are obtained under laboratory conditions. In addition, the quality of the microphone  
465 device has been proven to have little influence on the overall accuracy of this method. Furthermore,  
466 the distance from the nozzle tip to the microphone has not been shown to be overly influential, but  
467 the shortest distance does generally provide the most accurate results. Nevertheless, the results  
468 achieved in this article should be confirmed through field tests in agricultural environments. Deeper  
469 theoretical insight into acoustic signal generation in nozzle tips and its relationship with flow rate is  
470 also needed.

471

472 **Acknowledgments:** The tests conducted in this study could be performed thanks to two three-month-long  
473 visiting scholarships granted by the University of Valladolid to both Víctor Martínez-Martínez and Ruben  
474 Ruiz-Gonzalez. Furthermore, during all the stages of this study, they were both funded by a *Formación de*  
475 *Personal Investigador* program grant, financed by the *University of Valladolid* (Spain) and co-financed by *Banco*  
476 *Santander*. The authors would also like to express their sincere gratitude to the Writing Center of the University  
477 of Kentucky (USA), with a special mention to Leslie C. Davis, for their valuable help with the language editing  
478 and proofreading of the article.

479 **Author Contributions:** Timothy S. Stombaugh conceived the original idea; Timothy S. Stombaugh, Víctor  
480 Martínez-Martínez and Ruben Ruiz-Gonzalez designed the experiments; Ruben Ruiz-Gonzalez performed the  
481 experiments; Ruben Ruiz-Gonzalez and Víctor Martínez-Martínez proposed the acoustic estimation method  
482 and analyzed the experimental data under the supervision and guidance of Jaime Gomez-Gil and Timothy S.  
483 Stombaugh; all four coauthors collaboratively wrote the paper. All authors have approved the final version of  
484 this article.

485 **Conflicts of Interest:** The authors declare no conflict of interest.



486 **Abbreviations**

487 The following abbreviations are used in this manuscript:

488

489 DAQ: *Data Acquisition*

490 DFT: *Discrete Fourier Transform*

491 FFT: *Fast Fourier Transform*

492 IIR: *Infinite Impulse Response*

493 lpm: *liters per minute*

494 PSD: *Power Spectral Density*

495 PWM: *Pulse-Width Modulation*

496 RMSE: *Root Mean Square Error*

497 USB: *Universal Serial Bus*

498 **References**

499 [1] K.L. Hughes, A.R. Frost, A review of agricultural spray metering, *Journal of Agricultural Engineering*  
500 *Research*, 32 (1985) 197-207.

501 [2] D.J. Mulla, Twenty five years of remote sensing in precision agriculture: Key advances and remaining  
502 knowledge gaps, *Biosystems Engineering*, 114 (2013) 358-371.

503 [3] M. Loghavi, B. Behzadi Mackvandi, Development of a target oriented weed control system, *Computers and*  
504 *Electronics in Agriculture*, 63 (2008) 112-118.

505 [4] H. Nordmeyer, A. Hausler, P. Niemann, Patchy weed control as an approach in precision farming, in:  
506 *Precision Agriculture 1997. Proceedings of the 1<sup>st</sup> European Conference on Precision Agriculture, 1997*, pp.  
507 307-314.

508 [5] S. GopalaPillai, L. Tian, J. Zheng, Evaluation of a flow control system for site-specific herbicide applications,  
509 *Transactions of the ASAE*, 42 (1999) 863-870.

510 [6] R.B. Michael, J.B. Weber, R.S. Len, Efficacy of selected herbicides as influenced by soil properties, *Weed*  
511 *Technology*, 4 (1990) 279-283.

512 [7] L. Hui, Z. Heping, S. Yue, C. Yu, H.E. Ozkan, Development of digital flow control system for multi-channel  
513 variable-rate sprayers, *Transactions of the ASABE*, 57 (2014) 273-281.

514 [8] E. Gil, J. Llorens, J. Llop, X. Fàbregas, A. Escolà, J.R. Rosell-Polo, Variable rate sprayer. Part 2 – Vineyard  
515 prototype: design, implementation, and validation, *Computers and Electronics in Agriculture*, 95 (2013)  
516 136-150.

517 [9] Z. Zhang, L. Mongeau, S.H. Frankel, S. Thomson, J.B. Park, Sound generation by steady flow through  
518 glottis-shaped orifices, *The Journal of the Acoustical Society of America*, 116 (2004) 1720-1728.

519 [10] S.C. Sheen, Noise generated by multiple-jet nozzles with conical profiles, *International Journal of*  
520 *Occupational Safety and Ergonomics*, 17 (2011) 287-299.

521 [11] G.E. Cann, P. Leehey, The acoustic source created by turbulent flow over orifices and louvers,  
522 *Massachusetts Inst. of Tech., Cambridge: Report No. 97674* (June 1987).

523 [12] P. Testud, P. Moussou, A. Hirschberg, Y. Aurégan, Noise generated by cavitating single-hole and  
524 multi-hole orifices in a water pipe, *Journal of Fluids and Structures*, 23 (2007) 163-189.

525 [13] P. Testud, Y. Aurégan, P. Moussou, A. Hirschberg, The whistling potentiality of an orifice in a confined  
526 flow using an energetic criterion, *Journal of Sound and Vibration*, 325 (2009) 769-780.

527 [14] M.S. Howe, Mechanism of sound generation by low Mach number flow over a wall cavity, *Journal of*  
528 *Sound and Vibration*, 273 (2004) 103-123.

529 [15] P. Druault, X. Gloerfelt, T. Mervant, Investigation of flow structures involved in sound generation by two-  
530 and three-dimensional cavity flows, *Computers & Fluids*, 48 (2011) 54-67.

- 531 [16] T. Kobayashi, T. Takami, M. Miyamoto, K. Takahashi, A. Nishida, M. Aoyagi, 3D calculation with  
532 compressible LES for sound vibration of ocarina, in ArXiv e-prints, 2009.
- 533 [17] H. Jacobs, Y. Skibbe, M.J. Booyesen, C. Makwiza, Correlating sound and flow rate at a tap, *Procedia*  
534 *Engineering*, 119 (2015) 864-873.
- 535 [18] H. Kakuta, K. Watanabe, Y. Kurihara, Development of vibration sensor with wide frequency range based  
536 on condenser microphone - Estimation system for flow rate in water pipes, *World Academy of Science,*  
537 *Engineering and Technology - International Journal of Mechanical, Aerospace, Industrial, Mechatronic and*  
538 *Manufacturing Engineering*, 6 (2012) 2267-2272.
- 539 [19] Teejet®, webpage of the nozzle tips manufacturer. <http://www.teejet.com/> (accessed on 27 February 2017).
- 540 [20] Wilger Industries Ltd., webpage of the nozzle tips manufacturer. <http://www.wilger.net/> (accessed on 27  
541 February 2017).
- 542 [21] R.P. Evans, J.D. Blotter, A.G. Stephens, Flow rate measurements using flow-induced pipe vibration, *Journal*  
543 *of Fluids Engineering*, 126 (2004) 280-285.
- 544 [22] M. Kohlmann, Selecting the right flowmeter for the job, *Chemical Engineering*, 111 (2004) 60-64.
- 545 [23] Liquid flowmeters – A guide for selecting a flowmeter for pressurized systems.  
546 <http://www.ecy.wa.gov/programs/wr/measuring/images/pdf/gsfps.pdf> (accessed on 27 February 2017).  
547